Oscillations and Complex Mechanisms: O_2 Oxidation of Benzaldehyde

M. G. Roelofs,*† E. Wasserman,*† and J. H. Jensen‡

Contribution No. 4189 from the Central Research and Development Department and the Agricultural Products Department, E. I. du Pont de Nemours & Company, Wilmington, Delaware 19898. Received September 29, 1986

Abstract: The oxidation of benzaldehyde catalyzed by cobalt and bromine is an oscillating reaction in which the concentrations of Co(III) and of dissolved oxygen vary periodically with time. A mechanistic model is proposed in which the reaction alternates between two stages. In stage I the dissolved oxygen concentration is appreciable and benzoyl radicals combine with oxygen, ultimately oxidizing Co(II) to Co(III). In stage II dissolved oxygen is depleted, and benzoyl radicals are oxidized by Co(III). The model gives satisfactory agreement with a number of qualitative and quantitative features. These include the composition of the steady states and the amplitude and period of oscillation for different concentrations of cobalt, bromide, and benzaldehyde. Specific measurements were also made of the kinetics of the reduction of cobalt(III) by mixtures of benzaldehyde and sodium bromide, the stability of a cobalt–bromide complex, and the consumption of $^{18}O_2$. This last study demonstrates the presence of two major pathways to benzoic acid which differ in the source of oxygen.

The reactions of O_2 with organics can be complex and difficult to elucidate. This study employs oscillatory behavior to assist in understanding one such oxidation. The program arose as a combination of two efforts. The catalyzed oxidation of benzaldehyde to benzoic acid was discovered to be oscillatory, an organic oscillating system.[1] Independently, conjectures were raised that new oscillating chemistry might be found in the O_2 oxidations of organic compounds.[2] If so, novel modes of kinetic behavior would be obtained for a major class of reactions. Such oxidative systems might also lead to fresh mechanistic insights as the details of oscillations are often sensitive to many reaction parameters. Oscillations can reflect the interaction of a number of elementary steps and thus provide a broad view of the underlying chemistry.

A preliminary communication proposed a free-radical mechanism for the oscillations during benzaldehyde oxidation.[3] Here we present a substantially expanded experimental investigation and an elaborated mechanism. To us, the work reported indicates that new mechanistic information may indeed be available from the examination of a complex system in an oscillating mode. Catalyzed O_2 oxidations of benzaldehyde had received extensive study as a prototypical oxidation,[4,5] yet this investigation of the oscillations has led to increased understanding.

Typical initial concentrations are 750 mM benzaldehyde, 20 mM cobaltous acetate, and 10 mM sodium bromide. Oscillations occur in the acetic acid/water solutions at 70 °C when air or oxygen contacts the solution. Figure 1 shows the redox potential superimposed on the optical absorption largely due to Co(III). The potential and the logarithm of the Co(III) concentration rise slowly until they reach a maximum. The potential then decreases rapidly, the color changing from the dark olive green characteristic of Co(III) in acetic acid to the pale pink of Co(II). The approximately linear increase in log [Co(III)] points to an autocatalytic reaction, a feature often found in chemical oscillators.

The dissolved oxygen concentration is compared with the potential in Figure 2. In this experiment the period of oscillations was increased over that in Figure 1 by using a lower concentration of bromide ion. Under these conditions the oscillations can be cleanly divided into two stages. In stage I the oxygen concentration is appreciable and the potential (and thus [Co(III)]) increases. In stage II no dissolved oxygen is detected (less than 0.5% of saturation) and the potential decreases.

To obtain an overview of the suggested mechanism of oscillation let us consider the following three net processes for producing benzoic acid:

$$\mathrm{PhCHO} + \mathrm{O_2(l)} + 2\mathrm{Co(II)} + 2\mathrm{H^+} \rightarrow \mathrm{PhCO_2H} + 2\mathrm{Co(III)} + \mathrm{H_2O} \quad \text{(A)}$$

$$\mathrm{PhCHO} + 2\mathrm{Co(III)} + \mathrm{H_2O} \rightarrow \mathrm{PhCO_2H} + 2\mathrm{Co(II)} + 2\mathrm{H^+} \quad \text{(B)}$$

$$2\mathrm{PhCHO} + \mathrm{O_2(l)} \rightarrow 2\mathrm{PhCO_2H} \quad \text{(C)}$$

$$\mathrm{A} + \mathrm{B} = \mathrm{C}$$

Formally, the O_2 oxidation may be viewed as process C. However, a complication arises in a two-electron oxidation of aldehyde to acid using the four-electron oxidant O_2. With A, the extra 2 equiv oxidize Co(II). But if cobalt is to act catalytically, the Co(III) produced in A must be destroyed in B. Under the conditions of oscillation processes A and B do not proceed simultaneously but alternate.

At low cobalt(III) concentrations, the rate of oxygen consumption is smaller than the rate of oxygen transfer from the gas phase to the liquid. Thus, at the beginning of stage I the concentration of dissolved oxygen is increasing. The stoichiometry approximates that of process A, an autocatalytic reaction which accelerates as more Co(III) is produced. The maximum in dissolved oxygen occurs when its consumption through A is balanced by its dissolution. As A continues to accelerate, oxygen is consumed faster than supplied so that the reservoir in solution is ultimately depleted. The rate of A is comparatively insensitive to changes in oxygen concentration at medium to high levels; the consequences of its exhaustion occur suddenly and mark the end of stage I.

As the dissolved oxygen is depleted, the cobalt(III) concentration reaches a maximum. The chemistry switches to process B. The reduction of Co(III) is here mediated by a high concentration of free radicals, which are no longer scavenged by dissolved oxygen. The store of cobalt(III) created during stage I is consumed in a rapid oxidation of benzaldehyde. During stage II, the bulk liquid remains essentially depleted of oxygen. At the gas/liquid interface the oxygen reacts rapidly with the high concentration of free radicals. These reactions continue until

†Central Research and Development Department.
‡Agricultural Products Department.

(1) Jensen, J. H. *J. Am. Chem. Soc.* **1983**, *105*, 2639–2641.
(2) Wasserman, E.; Druliner, J. D.; Roelofs, M. G.; Greller, L., to be published.
(3) Roelofs, M. G.; Wasserman, E.; Jensen, J. H.; Nader, A. E. *J. Am. Chem. Soc.* **1983**, *105*, 6329–6330. Note that the labeling of mechanistic steps R_i is not the same in the present paper and this reference.
(4) (a) Bawn, C. E. H.; Jolley, J. E. *Proc. R. Soc. London, A.* **1956**, *237*, 297–312. (b) Marta, F.; Boga, E.; Matok, M. *Discuss. Faraday Soc.* **1968**, *46*, 173–183.
(5) Hendriks, C. F.; von Beek, H. C. A.; Heertjes, P. M. *Ind. Eng. Chem. Res. Div.* **1978**, *17*, 260–264.

0002-7863/87/1509-4207$01.50/0

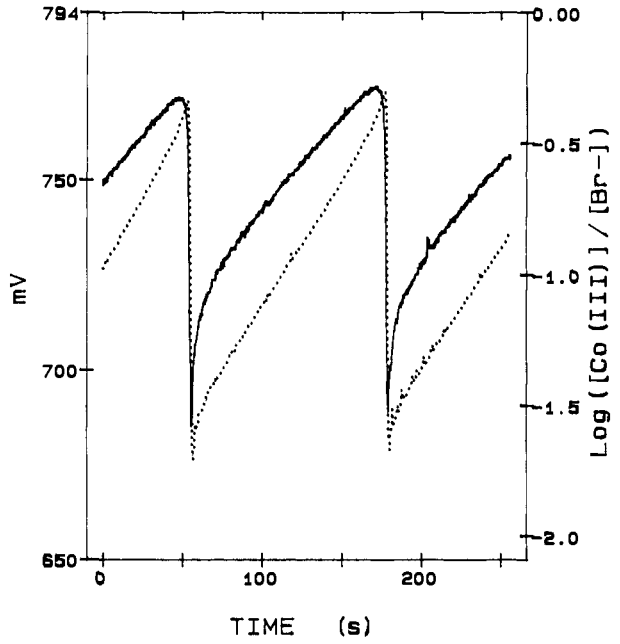

Figure 1. Oscillations in the potential (solid line) of a platinum electrode vs. Ag/AgCl reference electrode and log ([Co(III)]/[Br⁻]) determined from optical absorption (dotted line). Conditions are as described in the Experimental Section, except [Br⁻] is taken at a constant 15 mM. Data were collected 32 min after the addition of benzaldehyde in a batch reaction. The vertical scales are adjusted so that E = 794 + 69 log ([Co(III)]/[Br⁻]).

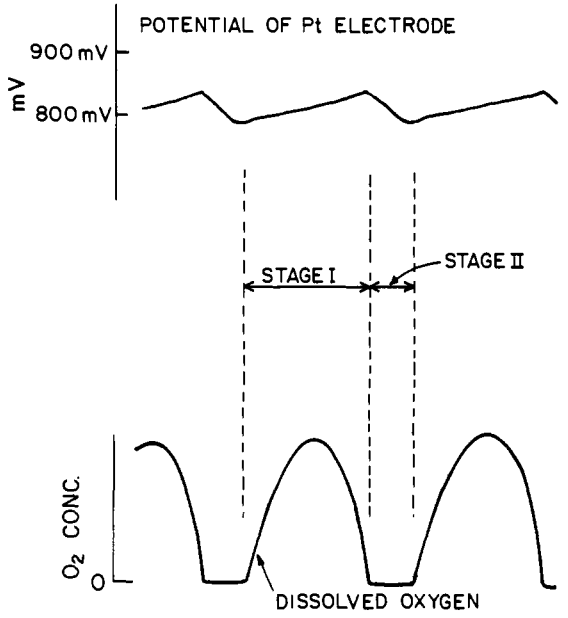

Figure 2. Comparison of the potential of the Pt electrode with the dissolved oxygen concentration in a batch reaction. [O_2(l)] reaches a maximum of 25% saturation with O_2(g) at 1 atm. Conditions are as described in the Experimental Section, except of [Br⁻] = 2 mM.

cobalt(III) is exhausted. Then the last of the radicals are destroyed as oxygen sweeps back into the bulk solution. Stage I begins again.

After discussing the experimental methods, this report describes some of the components of the oscillator. We consider oxidation of Co(II) by peracid, rearrangements of Co(III) complexes, production of hypobromous acid and bromine, cobalt(II)–bromide complexes, reductions of cobalt(III) by benzaldehyde and bromide, O_2 solubility and dissolution rates, and reactions requiring O_2. The kinetic model derived from these studies is summarized in Table I. Next we present observations on the oscillatory system and compare them with some predictions of the model. These include bromide, benzaldehyde, and benzoic acid concentrations, as well as the effects of additions of perbenzoic acid, oxygen labeling, and changes of the concentrations of cobalt, bromide, or benzaldehyde.

Table I. Model for Benzaldehyde Oxidation[a]

$2Co(II) + RCO_3H + 2H^+ \rightarrow Co(III)_2 + RCO_2H + H_2O$	D1
$Co(III)_2^s \rightleftarrows Co(III)_2^c$	D2
$Br^- + PhCO_3H + H^+ \rightarrow PhCO_2H + HOBr$	D3
$Co(III)_2^s + Br^- + H_2O \rightleftarrows 2Co(II) + HOBr + H^+$	D4
$HOBr + Br^- + H^+ \rightleftarrows Br_2 + H_2O$	D5
$Co(III)_2^sPhCHO \rightarrow Co(III)_2^cPhCHO$	D6
$Co(III)_2^c + PhCHO \rightleftarrows Co(III)_2^cPhCHO$	D7
$Co(III)_2^cPhCHO \rightarrow PhCO^\bullet + H^+ + Co(II) + Co(III)$	D8
$PhCO^\bullet + Co(III)_2^c + H_2O \rightarrow PhCO_2H + Co(II) + H^+ + Co(III)$	D9
$PhCO^\bullet + Co(III)_2^cPhCHO + H_2O \rightarrow PhCO_2H + Co(II) + H^+ + Co(III) + PhCHO$	D10
$2Co(II)Br^\bullet \xrightarrow{fast} Br_2 + 2Co(II)$	D11
$Co(II)Br^\bullet + Co(III)_2^s + H_2O \xrightarrow{fast} HOBr + 2Co(II) + H^+ + Co(III)$	D12
$Co(II) + PhCO_3H \underset{k_{-1}}{\overset{k_1}{\rightleftarrows}} Co(II)PhCO_3H$	R1
$k_1 = 0.1 \times 10^6\ M^{-1}\ s^{-1}$; $k_1 = 0.1 \times 10^5\ s^{-1}$	
$Co(II)PhCO_3H + Co(II) + 2H^+ \rightarrow Co(III)_2^s + PhCO_2H + H_2O$	R2
$k_2 = 0.2 \times 10^6\ M^{-1}\ s^{-1}$	
$Co(III)_2^s + PhCHO \rightleftarrows Co(III)_2^sPhCHO$	R3
$k_3 = 0.54 \times 10^1\ M^{-1}\ s^{-1}$; $k_{-3} = 0.1 \times 10^1\ s^{-1}$	
$Co(III)_2^sPhCHO \rightarrow PhCO^\bullet + Co(II) + H^+ + Co(III)$	R4
$k_4 = 0.17 \times 10^{-2}\ s^{-1}$	
$PhCO^\bullet + Co(III)_2^s + H_2O \rightarrow PhCO_2H + Co(II) + H^+ + Co(III)$	R5
$k_5 = 0.1 \times 10^2\ M^{-1}\ s^{-1}$	
$PhCO^\bullet + Co(III)_2^sPhCHO + H_2O \rightarrow PhCO_2H + Co(II) + H^+ + Co(III) + PhCHO$	R6
$k_6 = 0.1 \times 10^2\ M^{-1}\ s^{-1}$	
$2Co(III) \rightarrow Co(III)_2^s$	R7
$k_7 = 0.1 \times 10^5\ M^{-1}\ s^{-1}$	
$Co(III)_2^s + Br^- \rightleftarrows Co(III)_2Br^-$	R8
$k_8 = 0.1 \times 10^4\ M^{-1}\ s^{-1}$; $k_{-8} = 0.1 \times 10^4\ s^{-1}$	
$Co(III)_2Br^- \rightarrow Co(III) + Co(II)Br^\bullet$	R9
$k_9 = 0.87\ s^{-1}$	
$Co(II)Br^\bullet + PhCHO \rightarrow PhCO^\bullet + Co(II) + H^+ + Br^-$	R10
$k_{10} = 0.1 \times 10^4\ M^{-1}\ s^{-1}$	
$Co(III)_2^sPhCHO + Br^- \rightleftarrows Co(III)_2PhCHOBr^-$	R11
$k_{11} = 0.1 \times 10^4\ M^{-1}\ s^{-1}$; $k_{-11} = 0.1 \times 10^4\ s^{-1}$	
$Co(III)_2PhCHOBr^- \rightarrow PhCO^\bullet + Co(II) + H^+ + Co(III) + Br^-$	R12
$k_{12} = 0.87\ s^{-1}$	
$PhCO^\bullet + Co(III)_2Br^- + H_2O \rightarrow PhCO_2^\bullet + 2Co(II) + 2H^+ + Br^-$	R13
$k_{13} = 0.81 \times 10^6\ M^{-1}\ s^{-1}$	
$PhCO^\bullet + Co(III)_2PhCHOBr^- + H_2O \rightarrow PhCO_2^\bullet + 2Co(II) + 2H^+ + Br^- + PhCHO$	R14
$k_{14} = 0.81 \times 10^6\ M^{-1}\ s^{-1}$	
$PhCO_2^\bullet + PhCHO \rightarrow PhCO_2H + PhCO^\bullet$	R15
$k_{15} = 0.1 \times 10^8\ M^{-1}\ s^{-1}$	
$PhCO_2^\bullet + Co(II) \rightarrow PhCO_2H + Co(III)$	R16
$k_{16} = 0.75 \times 10^5\ M^{-1}\ s^{-1}$	
$O_2(g) \rightleftarrows O_2(l)$	R17
$k_{17} = 0.15 \times 10^{-3}\ M\ atm^{-1}\ s^{-1}$; $k_{-17} = 0.25 \times 10^{-1}\ s^{-1}$	
$PhCO^\bullet + O_2(l) \rightarrow PhCO_3^\bullet$	R18
$k_{18} = 0.5 \times 10^9\ M^{-1}\ s^{-1}$	
$PhCO_3^\bullet + PhCHO \rightarrow PhCO^\bullet + PhCO_3H$	R19
$k_{19} = 0.4 \times 10^4\ M^{-1}\ s^{-1}$	
$PhCO_3^\bullet + Co(II) + H^+ \rightarrow PhCO_3H + Co(III)$	R20
$k_{20} = 0.8 \times 10^5\ M^{-1}\ s^{-1}$	
$PhCO_3^\bullet + PhCO^\bullet \rightarrow 2PhCO_2^\bullet$	R21
$k_{21} = 0.8 \times 10^8\ M^{-1}\ s^{-1}$	

[a] Only reactions R1–R21 are included in the kinetic model for oscillations. Reactions D1–D12 are discussed in the text. The scheme referred to in the text consists of reactions D2, D6–D10, and R3–R7. [b] $[PhCHO]_o$ = 750 mM, $[Br^-]_o$ = 10 mM, $[Co(II)]_o$ = 20 mM, [O_2(g)] = 1 atm (held constant), and residence time = 900 s.

Experimental Methods

The reaction vessel usually was a six-neck 250-mL round-bottom flask fitted with a thermometer, thermocouple, and condenser. Air or oxygen

from a mass flow meter was introduced into the liquid through a fritted glass tube of medium porosity. Stirring was by an egg-shaped stir bar of 38-mm length magnetically driven at 600 rpm. Typical conditions were initial concentrations of 750 mM PhCHO, 20 mM $Co(AcO)_2 \cdot 4H_2O$, and 10 mM NaBr in a solvent of 90:10 w/w $AcOH/H_2O$, an oxygen flow rate of 20 sccm (standard cubic centimeters per minute), and a total liquid volume of 150 mL at 70 °C. Use of $Co(NO_3)_2 \cdot 6H_2O$ does not produce oscillations under these conditions.

The redox potential of the solution was monitored with a platinum electrode and a Ag/AgCl,KCl reference electrode. Alternatively, a bare silver wire immersed in the solution was quickly coated with silver bromide and can be used as the reference electrode provided that $[Br^-]$ remains constant. The difference in potential between the platinum and silver wires had nearly the same amplitude and shape of oscillations as was obtained with Ag/AgCl,KCl or calomel reference electrodes. In some cases, particularly at high temperatures, the silver wire is more convenient to use than external electrodes with liquid junctions. Absorption of light at 620 nm was measured with a Brinkman dipping probe colorimeter with a 1-cm path. Concentrations of Co(III) were calculated by using an extinction coefficient at 620 nm of 150 M^{-1} cm^{-1} (based on monomers). The contribution to absorption at 620 nm due to cobalt(II)–bromide complexes was assumed to be constant.

The bromide ion concentration was measured by using a Ag/AgBr,-Ag_2S electrode (Orion). In the absence of other added electrolytes, its calibration curve in $AcOH/H_2O$ is linear (slope = −58 mV/decade at 25 °C) from 10^{-6} to 10^{-3} M sodium bromide. Above 1 mM there is curvature in the calibration plot. In the presence of 100 mM $LiClO_4$ (to maintain constant ionic strength) the curve remains linear up to at least 0.1 M. The deviations below 10^{-6} M are due to solubility of silver bromide in $AcOH/H_2O$. For the oscillating reaction, bromide ion concentrations were obtained with a calibration curve constructed at 70 °C by using stock solutions of sodium bromide in $AcOH/H_2O$.

The dissolved oxygen concentration was measured with a Clark-type electrode (Altex No. 531192). The device contains a gold electrode covered with a thin film of electrolyte and then a Teflon membrane. A potential sufficient to reduce dioxygen is applied to the gold electrode, making the concentration of oxygen at the electrode surface nearly zero. Oxygen diffuses from the solution through the membrane and to the electrode with a flux proportional to its partial pressure in solution. No interference was found from Co(II), Co(III), Br^-, or Br_2.

HPLC analyses were performed by using a Du Pont Zorbax ODS column of 15-cm length, a column temperature of 35 °C, a carrier of 55:45:0.1 $CH_3CN/H_2O/CF_3CO_2H$, and a detection wavelength of 272 nm. Perbenzoic acid was prepared by the method of Kolthoff et al.[6] After acidification, the peracid was extracted into ether, the ether combined with 90:10 $AcOH/H_2O$, and most of the ether removed by rotary evaporation.

For measuring the dependence on reactant concentrations, a continuous-feed stirred tank reactor (CSTR) was used. A preheated solution containing Co(II), Br^-, and PhCHO was pumped into the flask at 10 mL min^{-1} (flow rate/volume = 1.11×10^{-3} s^{-1}), and reactor liquid was drained at the same rate.

Elements of the Model

Co(III) Production from Peracid. There has been some controversy over the structure of cobaltic ions in solution. Kinetic[7] spectrophotometric,[8] and ^{18}O-labeling[9] studies had shown that in dilute aqueous perchloric acid solutions (<0.1 M H^+) cobalt(III) is present primarily as a dimer. By use of molecular weight determination by freezing point depression in anhydrous acetic acid, two groups[10,11] also formulate cobaltic acetate as a hydroxide-bridged dimer of composition $Co_2(OAc)_4(OH)_2$. Others have reported the predominance of Co(III) monomers[12] or a mixed-valence trimer containing two Co(III)'s and one Co(II).[13] It is likely that cobaltic acetate is a mixture of several of these complexes, though the dimeric form may well dominate under our conditions. In order to keep the model which follows relatively simple, all reactions of Co(III) are assumed to occur with dimers. The use of dimers, however, is not critical. They can be replaced by monomers and still maintain oscillations.

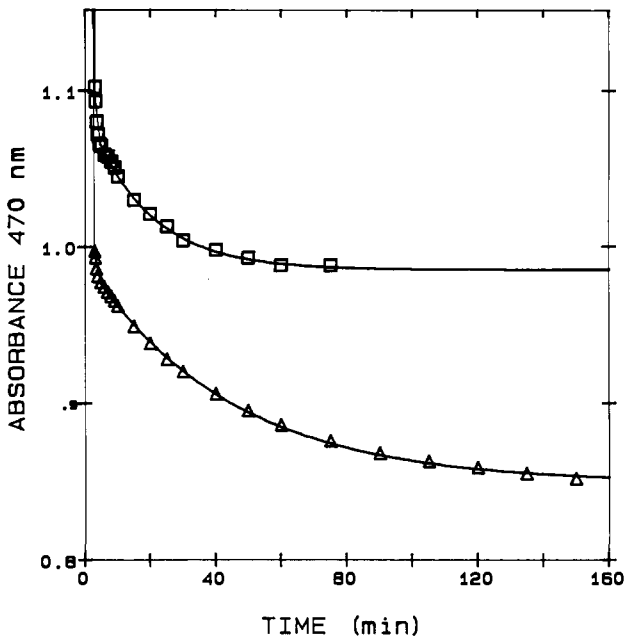

Figure 3. Absorbance changes at 470 nm (1-cm path length) following the oxidation of Co(II) at 70 °C by MCPBA which is 2 mM before reaction. Total cobalt concentrations after the addition of MCPBA are 40 (squares) or 80 mM (triangles). Solid lines are the sum of two exponentials. The decay rate of the fast component is 0.047 s^{-1} for both curves. The slow component arises from the rearrangement $Co(III)_2^s \rightarrow Co(III)_2^c$ with rate 3.8×10^{-4} s^{-1} at 36 mM Co(II) and 9.1×10^{-4} s^{-1} at 76 mM Co(II).

Cobalt(III) can be formed in quantitative yield by oxidation of Co(II) with organic peracids[11,14] (reaction D1 of Table 1): Using the stopped-flow method, Jones studied this reaction in 95:5 w/w $AcOH/H_2O$ with *m*-chloroperbenzoic acid (MCPBA) as oxidant. He found that (a) the rate of the reaction is first order in per acid and second order in Co(II), (b) the activation energy is 40 kJ mol^{-1}, and (c) increasing the water from 5% to 10% decreases the rate by a factor of 5.[15] This last change emphasizes the strong dependence on small variations of water content. The observations are consistent with rapid formation of a complex between Co(II) and peracid followed by rate-limiting attack of Co(II) on the complex, as in reactions R1 and R2 of Table I. Extrapolation to 70 °C in 90:10 $AcOH/H_2O$ shows the product k_1k_2/k_{-1} would be about 2×10^6 M^{-2} s^{-1}.[16] We verified the stoichiometry of two Co(III)'s formed from one perbenzoic acid. Also, compared to the oscillations, the reaction with that per acid is fast. The rate for perbenzoic acid is assumed equal to that for MCPBA given above.

A serious complication of Co(III) chemistry in acetic acid is rearrangement of the initial oxidation products into more stable Co(III) complexes. At 0 °C, the Co(III) initially produced from peracids has an apple-green color, is kinetically fast in reactions with reductants, and has been denoted as the dimer, $Co(III)_2^a$ (active).[14,15] Transformation occurs to an olive-green complex denoted $Co(III)_2^s$ (stable) which is kinetically slower in reactions with reductants. The $Co(III)_2^a \rightarrow Co(III)_2^s$ rearrangement is catalyzed by Co(II) and has a half-life of 32 s at 10 mM Co(III), 10 mM Co(II), 95% AcOH, and 20 °C. At 70 °C, the rearrangement has an exponential decay time of about 1 s. $Co(III)_2^s$

(6) Kolthoff, I. M.; Lee, T. S.; Mairs, M. A. *J. Polym. Sci.* **1947**, *2*, 199–205.
(7) Baxendale, J. H.; Wells, C. F. *Trans. Faraday Soc.* **1957**, *53*, 800–812.
(8) Sutcliffe, L. H.; Weber, J. R. *J. Inorg. Nucl. Chem.* **1960**, *2*, 281–286.
(9) Anbar, M.; Pecht, J. *J. Am. Chem. Soc.* **1967**, *89*, 2553–2556.
(10) Lande, S. S.; Falk, C. D.; Kochi, J. K. *J. Inorg. Nucl. Chem.* **1977**, *33*, 4104–4109.
(11) Koubek, E.; Edwards, J. O. *J. Inorg. Nucl. Chem.* **1963**, *25*, 1401–1408.
(12) Hendriks, C. F.; von Beek, H. C. A.; Heertjes, P. M. *Ind. Eng. Chem. Prod. Res. Div.* **1979**, *18*, 43–46.
(13) Ziolkowski, J. J.; Pruchnik, F.; Szymanska-Buzar, T. *Inorg. Chim. Acta* **1973**, *7*, 473–476.
(14) Jones, G. H. *J. Chem. Soc., Chem. Commun.* **1979**, 536–537.
(15) Jones, G. H. *J. Chem. Res., Synop.* **1981**, 228–229; *J. Chem. Res., Miniprint* **1981**, 2801–2868.
(16) We reserve k_i for the rate constant of the forward reaction R_i; k_{-i} for the reverse of R_i, and $K_i = k_i/k_{-i}$. Reactions labeled R_i will be included in the kinetic model for oscillations; those labeled D_i will not.

can also form a mixed-valence complex with Co(II) to yield a (possibly trimeric) species denoted $Co(III)_2^c$ (complexed) which is even slower than $Co(III)_2^s$ in reduction reactions. The equilibration between $Co(III)_2^s$ and $Co(III)_2^c$ takes place with a rate of 2×10^{-3} s^{-1} at 10 mM Co(III), 80 mM Co(II), 95% AcOH, and 70 °C.[15]

Figure 3 shows the absorbance at 470 nm following the reaction of Co(II) with MCPBA in 90% AcOH at 70 °C. Initially the absorbance undergoes a small rapid decrease, followed by a larger and slower diminuition. The slower change is associated with the equilibration D2 between $Co(III)_2^s$ and $Co(III)_2^c$. The rate of approach to equilbrium ($k_{D2} + k_{-D2}$, treating these as pseudo first order in the Co(III) species) was measured as 3.8×10^{-4} s^{-1} in the presence of 36 mM Co(II) and 9.1×10^{-4} s^{-1} with 76 mM Co(II). These rates agree, after accounting for differences in water content, with the measurements of Jones.[15]

In the oscillating reaction, most of the cobalt(III) is destroyed in each cycle of oscillation (Figure 1). Given the rates of rearrangement, the Co(III) has largely rearranged from $Co(III)_2^a$ to $Co(III)_2^s$ during a period of 100 s, and a small amount has been converted to $Co(III)_2^c$. In modeling oscillations, $Co(III)_2^s$ will be considered the only Co(III) species present. Limitations in this simplification may arise from neglect of reactions of the very reactive $Co(III)_2^a$ during the short time before it rearranges to $Co(III)_2^s$. The defficiency increases under conditions of short period (<20 s) as more of the Co(III) is in the active form.

Hypobromous Acid, Bromine, and Cobalt(II)–Bromide Complexes. Hypobromous acid and bromine may be formed from bromide by oxidation with perbenzoic acid or cobalt(III), as in reactions D3 and D4. The reaction of peracid with bromide (D3) is slower than reaction with Co(II) (R1, R2), though we find that increasing water content or higher temperature raises the rate of D3 relative to R1 and R2. At 70 °C in 10% water the two reactions have similar rates. Hypobromous acid was found not to oxidize Co(II) and to be reduced slowly back to bromide by benzaldehyde with no catalysis of this reduction by Co(II) (details are in the supplementary material). A complete mechanism would include reactions D3 and D5, but we do not include them in this oscillatory model. Note that oscillations can be obtained at Co(II):Br ratios as high as 10:1 for which D1 = R1 + R2 is ~10 times faster than D3.

Spectrophotometric and potential measurements were used to characterize complexes between Co(II) and bromide. By use of cobaltous acetate and sodium bromide at 70 °C in 90:10 $AcOH/H_2O$, a 1:1 $Co(II)/Br^-$ complex was demonstrated, having an extinction coefficient of 50 M^{-1} cm^{-1} at 609 nm, a formation constant of 4.3 M^{-1}, and an enthalpy of formation of +19 kJ mol^{-1}. Decreased water or replacement of the acetate by perchlorate[17,18] increases the stability of bromide-containing complexes. The data and its analysis are contained in the supplementary material.

At the "typical" bromide concentration of 10 mM used in the oscillator, only 4% of the cobalt(II) is complexed. In the absence of specific evidence that $Co(II)Br^-$ is more reactive than Co(II) or that it yields unique, mechanistically important products, we neglect this complexing in the model. Recognition of the increased absorption at 620 nm due to $Co(II)Br^-$ was, however, necessary for interpretation of absorbance measurements described below.

Reduction of Cobalt(III) by Benzaldehyde. In the absence of added reductants, $Co(III)_2^s$ oxidizes 90% acetic acid with a first-order rate constant of 5×10^{-5} s^{-1} at 70 °C and an activation energy of 120 kJ mol^{-1}. In the presence of benzaldehyde and the absence of oxygen and at low Co(II) concentrations, the rate of disappearance of $Co(III)_2^s$ is approximately first order in $Co(III)_2^s$ (Figure 4). The rate of decay of absorbance A over the first two lifetimes can be fit to

$$\frac{dA}{dt} = \frac{-k_4[\text{PhCHO}]A}{K_3^{-1} + [\text{PhCHO}]}$$

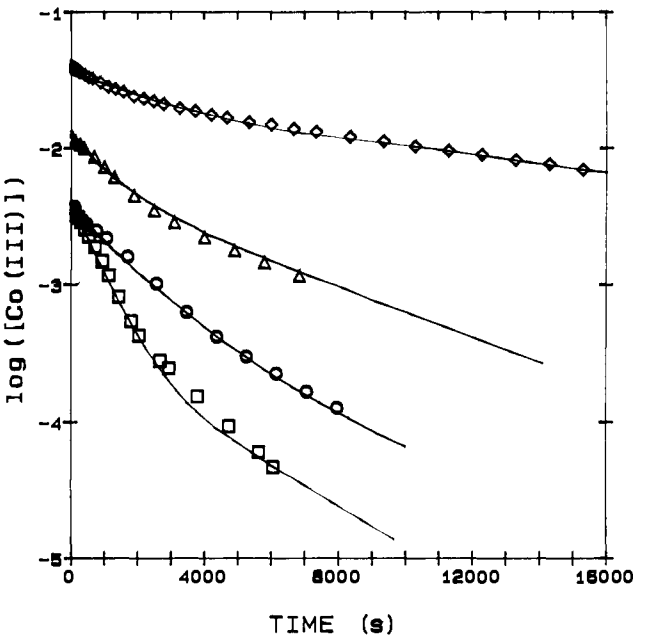

Figure 4. Reduction of Co(III) by benzaldehyde at 70 °C. Initial concentration of Co(III) was 4 mM (2 mM of $Co(III)_2$). Initial concentrations (in mM) of Co(II) and PhCHO were 16 and 100 (circles), 16 and 500 (squares), 36 and 500 (triangles), and 76 and 500 (diamonds). The data for 36 and 76 mM Co(II) have been shifted by a +0.5 and +1.0 (respectively) increase in the ordinate. Solid lines are calculated from the scheme described in the text and Table II.

Table II. Rate Constants for Reduction of Co(III) by Benzaldehyde

	conen of total Co, initial Co(III) (mM)	
	20, 4	40, 4
$1/K_3$ ($=1/K_{D7}$)	0.186 mM	0.145 mM
k_4	1.7×10^{-3} s^{-1}	8.4×10^{-4} s^{-1}
k_{D8}	3.4×10^{-4} s^{-1}	2.6×10^{-4} s^{-1}
k_{D2} ($=k_{D6}$)	8.0×10^{-5} s^{-1}	3.9×10^{-4} s^{-1}

At increasing Co(II) concentrations the decay becomes markedly nonexponential, characterized by an initial fast component followed by a slow component.

The major features of these decays can be accounted for with the kinetic scheme consisting of reactions D2, D6–D10, and R3–R7. Both $Co(III)_2^s$ and $Co(III)_2^c$ (see above) reversibly form a complex with benzaldehyde (R3, D7).[12] The extinction coefficient of the benzaldehyde complex is similar to that of $Co(III)_2^s$, so that the absorbance at 620 nm measures the total cobalt(III) concentration.[12] At low benzaldehyde concentrations the rate is first order in PhCHO, but above ~500 mM the rate becomes zero order, as essentially all $Co(III)_2^s$ is now complexed by R3. Both aldehyde complexes yield benzoyl radicals (R4, D8). Figure 4 is compatible with the $Co(III)_2^s$PhCHO complex forming benzoyl radicals more rapidly than $Co(III)_2^c$PhCHO, but note that initially only $Co(III)_2^s$ is present. Rearrangement of $Co(III)_2^s$ into the less reactive $Co(III)_2^c$ is assumed to occur at the same rate whether benzaldehyde is complexed to the cobalt or not (D2, D6). This rearrangement is catalyzed by Co(II) and results in the nonexponential decay of absorbance at high Co(II) concentrations. Any Co(III) species can oxidize the benzoyl radicals to benzoic acid (R5, R6, D9, D10).[5] Monomeric cobalt(III) is assumed to dimerize irreversibly (R7).

The above scheme was numerically integrated.[19] Deviations were determined of the calculated decays from experimental curves for different benzaldehyde concentrations at a fixed Co(II) concentration. An iterative minimizer program attached to the integrator then varied the rate constants seeking the best fits.[20] k_{D2}

(17) Sawada, K.; Tanaka, M. *J. Inorg. Nucl. Chem.* **1977**, *39*, 339–344.
(18) Sawada, K.; Nakamura, T.; Tanaka, M. *J. Inorg. Nucl. Chem.* **1980**, *42*, 1471–1475.
(19) Gear, C. W. *Numerical Initial Value Problems in Ordinary Differential Equations*; Prentice-Hall: Englewood Cliffs, NJ, 1971.

($=k_{D6}$) was constrained to the values found above for the $Co(III)_2^s$ rearrangement in the absence of benzaldehyde. Reactions R5, R6, D9, and D10 are assumed to be much faster than the others and have equal rate constants. These provide the correct overall stoichiometry of two Co(III)'s destroyed per initiation R4 or D8. K_3 was set equal to K_{D7}. With these assumptions there are three variable parameters (K_3, k_4, and k_{D8}) whose values are shown in Table II.

The rate constant for decomposition of $Co(III)_2^s$PhCHO (k_4) was found to be almost independent of Co(II) in the range of 2–10 mM, but increasing [Co(II)] from 16 to 36 mM decreased k_4 by a factor of 2. If the steps producing benzoyl radical, R4 and D8, are reversible, the models do not fit the data, as inhibition by Co(II) then occurs at all Co(II) concentrations. Instead, added cobaltous acetate, in addition to catalyzing D2, seems to produce an acid/base effect. Several metal acetates, including those with metal ions incapable of redox chemistry under our conditions, have been found to slow the rate of reduction of Co(III) in acetic acid. For example, KOAc, $Mg(OAc)_2$, and $Co(OAc)_2$ effect a similar slowing of the reduction of Co(III) by HBr.[15] Trifluoroacetic acid at 250 mM causes a fourfold increase in this rate.

The addition of 40 mM $Mg(OAc)_2$ to a solution (initial concentrations 4 mM Co(III), 16 mM Co(II), and 500 mM PhCHO) caused a decrease in the rate of decay of Co(III) by a factor of 2.4. Qualitatively, the addition of either cobaltous acetate or magnesium acetate also lowers the potential of a hydrogen ion electrode in 90% AcOH. Thus, the hydrogen ion/acetate equilibrium in 90% AcOH is not well buffered and can be shifted by metal acetate. This suggests that an intermediate in reductions of Co(III) is formed through a reversible loss of an acetate ligand or by protonation of a less reactive complex. Future kinetic studies of cobalt redox chemistry in $AcOH/H_2O$ might benefit from the explicit incorporation of an acetate buffer.

An alternative model also fits the Co(III) decay data reasonably well. Here $Co(III)_2^c$ is assumed to have no reactivity ($k_{D8} = 0$) but slowly oxidizes benzaldehyde through the reverse of D2 followed by R3 and R4. However, this model leads to rate constants for rearrangement of $Co(III)_2^s$ to $Co(III)_2^c$, k_{D2} ($=k_{D6}$), smaller than those found in the absence of benzaldehyde.

At a Co(II) concentration of 16 mM, the first-order decay time for equilibration between $Co(III)_2^s$ and $Co(III)_2^c$ is 280 min. For modeling oscillations with periods of several minutes, the production and subsequent slow reactions of $Co(III)_2^c$ will be ignored. Thus, D2 and D6–D10 will not be incorporated in the oscillatory model.

Reduction of Cobalt(III) by Bromide. Oxidation of bromide with Co(III) ultimately yields Br_2. In 90% AcOH at 70 °C and with excess bromide the reaction is sufficiently fast that $Co(III)_2^s$ is reduced before appreciable $Co(III)_2^c$ is formed. The decay of the Co(III) absorbance at 620 nm (dA/dt) is first order in Co(III) and first order in Br^-. In the presence of 16 mM Co(II) and with NaBr as the reductant, the rate can be expressed as

$$dA/dt = (-0.87\ M^{-1}\ s^{-1})[Br^-]A$$

Addition of 40 mM $Mg(OAc)_2$ to a solution containing 36 mM Co(II), 20 mM Br^-, and 4 mM Co(III) decreased the pseudo-first-order rate constant from 0.0130 to 0.0061 s^{-1}.

In a study of the oxidation of bromide by cobalt(III) in aqueous perchlorate, Wells et al. found a rate law first order in both Co(III) and Br^-.[21] They conclude that Co(III)–Br^- complexes are formed in rapid preequilibria followed by slow oxidation of the bromide. A similar mechanism consistent with the observations in 90% AcOH consists of reactions R8, R9, and D11 or R8–R9, D12, and D4. Production of free bromine atoms by cobaltic acetate has not been included here because the potential of the Co(III)/Co(II) couple in 90% acetic acid is about 1.2 V vs. SHE.

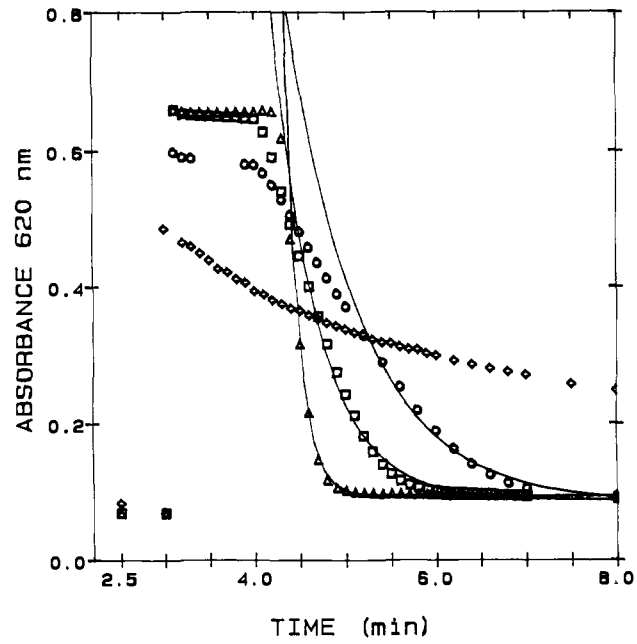

Figure 5. Reduction of Co(III) by PhCHO, catalyzed by Br^- at 70 °C. At 0 min 20 mM Co(II) is present. MCPBA is added at 3.0 min to give 4 mM Co(III). For three data sets PhCHO is present at 100 mM and 0 min while NaBr is added at 4.0 min to give these concentrations: 0.5 (circles), 1 (squares), and 2 mM (triangles). An experiment with no PhCHO and 5 mM Br^- present at 0 min (diamonds) yields a slow decay and demonstrates the synergistic effect of a combination of benzaldehyde and bromide. Solid lines are exponentials with decay rates of 0.020, 0.034, and 0.112 s^{-1} at $[Br^-]$ = 0.5, 1.0, and 2.0 mM, respectively.

Comparison with the estimated potential of the $Br^•/Br^-$ couple of 1.97 V[22] suggests that cobaltic acetate is not an oxidant of sufficient power to generate bromine atoms directly. The behavior of mixtures of Co(III), Br^-, and PhCHO did, however, indicate the formation of a species from Co(III) and Br^- which is capable of abstracting hydrogen from benzaldehyde (see next section). A bromine atom complexed to cobalt as in Co(II)Br• might be stabilized sufficiently to allow for its creation from bromide by cobalt(III) but still able to attack benzaldehyde. As in aqueous perchlorate, the oxidative step in complexed bromide (R9) is assumed to be irreversible. Otherwise, the order in Co(III) or Br^- could increase from 1 to 2. At this time we have no reason to choose between dimerization of one-electron oxidation products to form Br_2 (D11) or two-electron oxidation of bromide to hypobromous acid followed by oxidation of additional bromide (D12, D4).

Within the reproducibility of the data (15%), there is no deviation from a first-order dependence on Br^- up to 100 mM Br^-. Consequently, $1/K_8$ is taken as greater than 100 mM. This weak complexation is consistent with the difficulty of direct spectrophotometric observation of Co(III)–Br^- complexes.[15,21] The product K_8k_9 is taken to be 0.87 $M^{-1}\ s^{-1}$.

Mixtures of Co(III), Br^-, and PhCHO. Benzaldehyde and bromide act synergistically in the reduction of Co(III): the rate is much faster than with either reductant alone (Figure 5). A solution containing Co(II) and benzaldehyde was heated to slightly over 70 °C and deoxygenated with a stream of N_2. The absorbance is now due only to Co(II). MCPBA (0.1 M stock solution) and then NaBr (1.0 M stock solution) were injected, and the absorbance at 620 nm was recorded. Immediately after the injections, the temperature was within 1 °C of 70 °C, and a temperature controller maintained this value. The maximum rate of reduction of Co(III) does not occur immediately upon addition of bromide, rather there is a 10–40-s delay followed by an abrupt onset of decay. Once the reduction has started, it is not a simple exponential process, though the latter stages of it can often be

(20) McKinney, R. J.; Weigert, F. J., Quantum Chemistry Program Exchange, GEAR and ITERATOR available in VAX (522) and IBM-PC (QCMP022) versions.

(21) Wells, C. F.; Nazer, A. F. M.; Mays, D. *J. Inorg. Nucl. Chem.* **1977**, *39*, 2001–2005.

(22) Field, R. J.; Koros, E.; Noyes, R. M. *J. Am. Chem. Soc.* **1972**, *94*, 8649–8664.

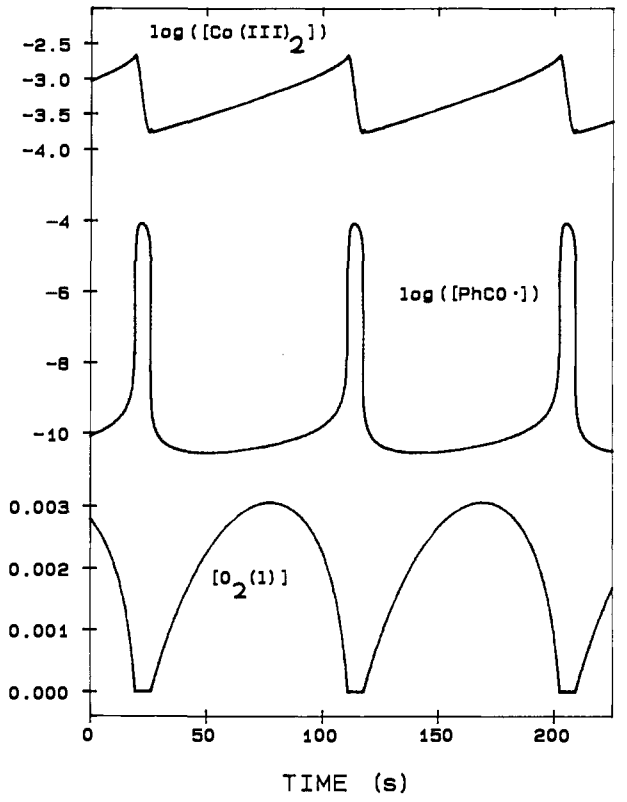

Figure 6. Oscillations calculated from model R1–R21 with the rate constants of Table I. The ordinate scales for $[Co(III)_2^s]$ and [PhCO•] are both $\log_{10}$ of concentration in mol/L, while that for $[O_2(l)]$ is linear in concentration.

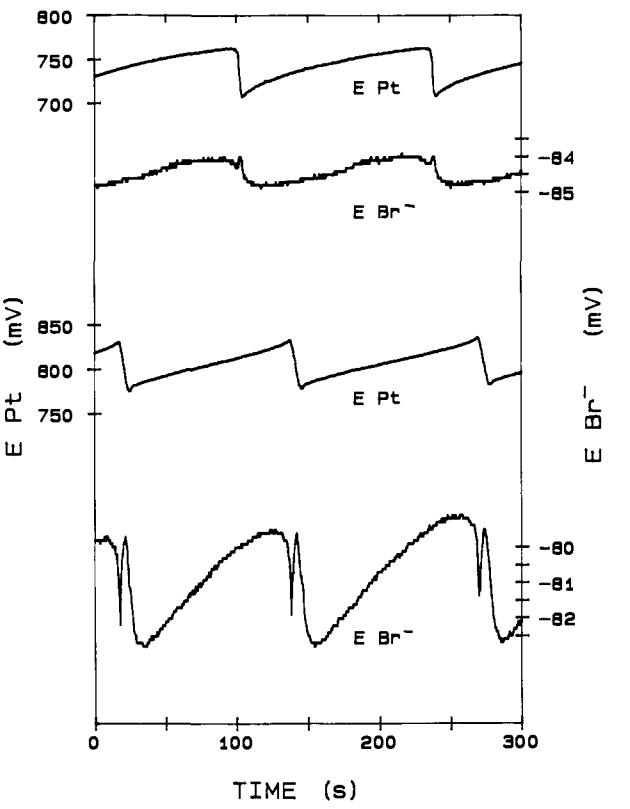

Figure 7. Comparison of the potential of a platinum electrode with that of a bromide ion selective electrode. The upper two traces are from a batch reaction in which air was fed to the reactor at 20 sccm, while the lower two traces were recorded from the same batch reaction 20 min after the air flow was replaced by an oxygen flow of 40 sccm.

approximated by an exponential.

The effect of added 2,6-di-*tert*-butyl-4-methylphenol (BHT), a radical scavenger, was studied. BHT is known to inhibit oxidation reactions by providing an easily abstractable hydrogen atom.[23] Oxy-centered radicals abstract this hydrogen, and the phenoxy radical thus formed does not continue the radical chain. Co(III) is reduced by BHT, but the (initial) decay rate at 4 mM Co(III) and 1 mM BHT is only 6×10^{-4} s^{-1}. Solutions containing 16 mM Co(II), 4 mM Co(III), 1 mM BHT, and 500 or 100 mM PhCHO exhibit a decay of Co(III) absorbance within 30% of the sum of the decay rates obtained from the aldehyde and the phenol separately. Thus the phenol does not greatly inhibit the oxidation of the benzaldehyde by Co(III) in the absence of bromide. In solutions containing initially 16 mM Co(II), 4 mM Co(III), 1 mM BHT, 100 mM PhCHO, and 1 mM Br$^-$, the rate of decay was 2.0×10^{-3} s^{-1}. This rate is 17 times less than the rate in the absence of the phenol (Figure 5), suggesting that the reduction of Co(III) by mixtures of PhCHO and Br$^-$ is a radical chain reaction involving oxy radicals as intermediates.

The rate of the Co(III)/PhCHO/Br$^-$ reaction is largely independent of benzaldehyde concentration above ~100 mM, reaching one-half of the maximum rate at 25 mM PhCHO. Between 0.5 and 3 mM Br$^-$ the rate is a quadratic function of [Br$^-$] (Figure 5). Measurements of the potential of the bromide-selective electrode during the reduction show that the major portion of the bromine remains as bromide, although some may be in other oxidation states or complexed to cobalt.

A mechanism consistent with these observations is R3–R16. Reactions R3–R9 have been previously introduced in the discussion of the separate reductions by benzaldehyde or bromide. In the presence of benzaldehyde, the intermediate in the oxidation of bromide by Co(III) (Co(II)Br•) yields a benzoyl radical (R10). An independence of coordination sites is assumed, so that a cobalt(III) dimer with a coordinated aldehyde can also complex with bromide. Thus, R11 is an analogue of R8 (with $K_{11} = K_8$) and R12 is an analogue of R9 and R10 (with $k_{12} = k_9$). The assumption of independence maintains the rate of benzoyl radical production in R9 and R10 as an increasing [PhCHO] transforms more $Co(III)_2^s$ to $Co(III)_2^s$PhCHO via R3.

A noteworthy element of this model is the overall two-electron oxidation of a benzoyl radical (R13 and analogue R14) by two cobaltic ions to produce a benzoyloxy radical. This is assumed to be catalyzed by bromine and could involve oxygen atom transfer to benzoyl from a coordinated hypobromite ion. Alternatively, two consecutive one-electron transfers with the same overall kinetics could be postulated. The two-electron oxidations (radical chain propagation) are in competition with the one-electron termination reactions (R5, R6). Benzoyloxy radicals abstract hydrogen from benzaldehyde in a propagation reaction (R15) in competition with their reduction by Co(II) in R16.

One case of interest occurs if [PhCHO] is sufficiently high so that R16 may be ignored in competition with R15, but the aldehyde still does not complex most $Co(III)_2^s$ by R3. Then the rate of reduction of $Co(III)_2^s$ is given by

$$\text{rate} = \frac{\text{initiation} \times \text{propagation}}{\text{termination}}$$

$$\text{rate} = (K_3k_4[\text{PhCHO}] + K_8k_9[\text{Br}^-]) \times [Co(III)_2^s]_t K_3k_{13}[Co(III)_2^s]_t[\text{Br}^-]/k_5[Co(III)_2^s]_t$$

$[Co(III)_2^s]_t$ is the sum of $[Co(III)_2^s]$ and $[Co(III)_2^s\text{PhCHO}]$. The initiation is linear in [Br$^-$], with a contribution at [Br$^-$] = 0 from $Co(III)_2^s$ and benzaldehyde reaction R4. The propagation rate is linear in [Br$^-$], resulting in an overall second-order dependence on [Br$^-$]. The dependence on $[Co(III)_2^s]_t$ is first order.

R3–R16 was numerically integrated and the rate of Co(III) reduction compared with experiment. The equilibrium constants K_3 and $K_8 = K_{11}$ and the rate constants k_4 and $k_9 = k_{12}$ were the same as those employed in the reductions by benzaldehyde or bromine alone. The reactions R7 and R10 have no competing reactions. Their rate constants are not important if they are

(23) Howard, J. A. *Adv. Free-Radical Chem.* **1972**, *4*, 49–173.

sufficiently fast to avoid significant accumulation of Co(III) monomer or Co(II)Br•. The ratio of the propagation constant k_{13} (=k_{14}) to the termination constant k_5 (=k_6) was adjusted at 1 M [PhCHO] and 1 mM [Br^-] until the rate of [$Co(III)_2$] decay was 0.045 s^{-1}. Then the ratio k_{15}/k_{16} was adjusted so that the rate was further reduced to 0.023 s^{-1} at 25 mM PhCHO (Table I).

Reactions Requiring Dioxygen. The Henry's law constant for oxygen in 90:10 AcOH/H2O at 70 °C was estimated as 3500 atm (mole fraction)$^{-1}$.[24-26] The time constant for equilibration of oxygen between the gas and liquid phases was measured to be 40 s. Transport of oxygen between gas and liquid was thus modeled by the equilibrium R17 with $k_{17} = 1.5 \times 10^{-4}$ M s^{-1} (atm O_2)$^{-1}$ and $k_{-17} = 0.025$ s^{-1}. Details are provided in the supplementary material.

In the autoxidation of benzaldehyde, benzoyl radicals combine with oxygen (R18), and the resulting benzoylperoxy radicals abstract hydrogen from benzaldehyde (R19).[23] Chain termination in autoxidation often occurs from dimerization of peroxy radicals.[27] However, the rate constants for oxidation by peroxy radicals of Co(II) complexes containing oxy ligands lie in the range 10^4–10^6 M^{-1} s^{-1} at 70 °C.[28-30] With the relatively high concentrations of Co(II) (>10^{-2} M), its reduction of benzoylperoxy (R20) is assumed to be the dominant mechanism of radical loss during stage I.

A series of numerical integrations of the differential equations associated with R1–R20 (using the rate constants of Table I), led to damped, but not sustained, oscillations. [$Co(III)_2^s$] grows exponentially in the presence of oxygen (R1–R4, R7–R12, R17–R20) and then decreases when O_2(l) is depleted (R3–R16). However, stage II is "weak", and the decrease of [$Co(III)_2^s$] is not sufficient to allow for replenishment of [O_2(l)].

The goal is to model the slow buildup of Co(III) during stage I followed by its fast decay in stage II. One might imagine that rapid creation and destruction of Co(III) occur continually with creation outweighing the destruction in stage I and the reverse in stage II. However, the corresponding consumption of benzaldehyde is then much higher than measured (Figure 8). Thus the rapid destruction of Co(III) is only "switched on" in stage II; it is not significant during stage I. Assuming that the initiation reactions producing benzoyl radicals are the same in stage I and stage II, stage II is faster because of a higher ratio of propagation/termination. The rate constants for the propagations of stage II, R13 and R14, can be increased until the termination reactions of stage II, R5 and R6, become insignificant, but R17–R18–R20 still provide a pathway for loss of benzoyl radicals. Increases in k_{13} and k_{14} or decreases in k_{20} insure rapid oxygen consumption even at low [$Co(III)_2^s$] and yield only a steady state with low [O_2(l)].

We thus propose an alternate fate for benzoylperoxy radicals during stage II involving reaction with benzoyl radical in R21. If the rate constant k_{21} is adjusted so that the increased benzoyl radical concentration allows R21 to compete with R20, sustained oscillations are obtained.

R21 should be thermodynamically allowed. The gas-phase heats of formation at 298 K ($\Delta H_f°$) of the benzoyl and benzoyloxy radicals are 66 and −82 kJ mol^{-1}, respectively.[31] By use of the group additivity principles, $\Delta H_f°$ for perbenzoic acid is calculated as −216 kJ mol^{-1}.[32] With the assumption that the O–H bond dissociation energy in perbenzoic acid is the same as in hydrogen peroxide (377 kJ mol^{-1}),[33] $\Delta H_f°$ of the benzoylperoxy radical is estimated as −58 kJ mol^{-1}. Thus R21 has an estimated enthalpy change of −170 kJ mol^{-1}. Production of benzoyl peroxide would be even more thermodynamically favored, though it was not detected by HPLC (concn < 300 μM). When added to the oscillator it was relatively stable, having a lifetime of 100 min. Formation of the $PhCO_3$–COPh bond could create 304 kJ mol^{-1} of vibrational energy. The occurrence of R21 would then require some of this energy (133 kJ mol^{-1}) to be used to break the O–O bond. Alternatively, both radicals may be complexed to cobalt so that formation of the $PhCO_2$–O_2CPh bond is avoided. Note that both R13 and R21 can be considered oxygen atom transfers to benzoyl radical. Alternative mechanisms which do not involve R21 are being considered.[34]

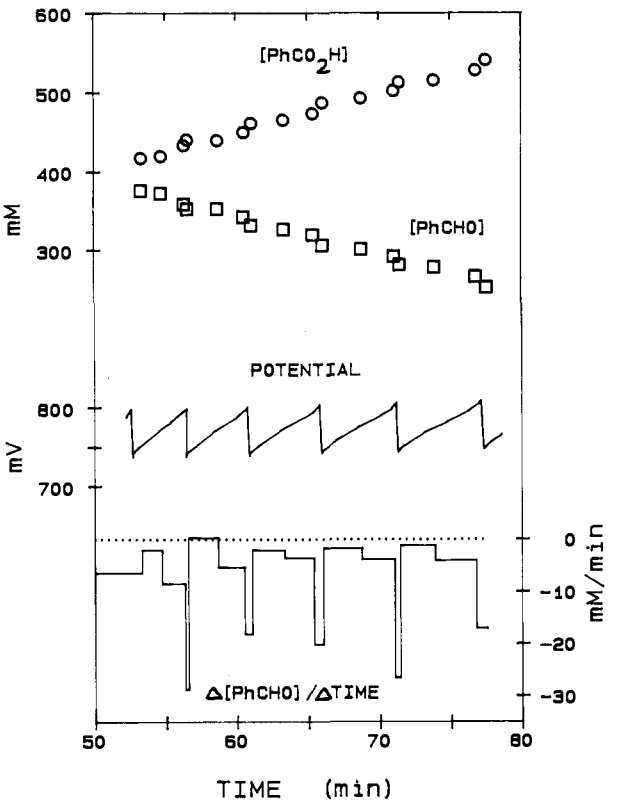

Figure 8. Concentrations of PhCHO (circles) and $PhCO_2H$ (squares), potential of Pt vs. Ag/AgCl (solid line), Δ[PhCHO]/Δtime (solid line), and the constant Δ[PhCHO]/Δtime = 0 (dots). Time scale is in minutes after the addition of benzaldehyde to a batch reaction under conditions given in the Experimental Section.

The rate of R18 is assumed to be somewhat less than diffusion controlled. The ratio k_{19}:k_{20} was adjusted to reproduce the observed rate of increase of [$Co(III)_2^s$] in stage I. k_{21} was adjusted until the calculated amplitude of oscillation was similar to that observed. The results of the calculation in Figure 6 should be compared with the experimental data in Figures 1 and 2.

Interpretation of the Potential of Pt. In the oscillatory system, significant quantities of Co(III) and Br^- exist simultaneously, though the thermodynamically favored products are Co(II) and Br_2. The Co(III)/Co(II) and Br_2/Br^- redox couples are not at equilibrium, and the potential of the platinum electrode may be a mixed potential, dependent upon the kinetics of reactions at the electrode surface. The potential (vs. Ag/AgCl, KCl) of freshly prepared mixtures of Co(III), Co(II), and Br^- with little Br_2 formed was found to follow the equation

$$E = 794 \text{ mV} + 78 \log ([Co(III)]/[Br^-])$$

(24) O'Connell, J. P. *ACS Symp. Ser.* **1977**, *60*, 490–497.
(25) Rudas, A. E. et al. *Tr. Nauchno-Issled. Inst. Proekt. Monomerov* **1974**, *4*, 143–147.
(26) Wilhelm, E.; Battino, R.; Wilcock, R. J. *Chem. Rev.* **1977**, *77*, 219–259.
(27) Sheldon, R. A.; Kochi, J. K. *Metal-Catalyzed Oxidations of Organic Compounds*; Academic: New York, 1981.
(28) Aleksandrov, A. L.; Solov'ev, G. I.; Denisov, E. T. *Izv. Akad. Nauk. SSSR, Ser. Khim.* **1972**, *7*, 1527–1533.
(29) Denisov, E. T. *Russ. Chem. Rev.* **1971**, *40*, 24–32.
(30) Howard, J. A.; Tong, S. B. *Can. J. Chem.* **1980**, *58*, 1962–1965.
(31) O'Neal, H. E.; Benson, S. W. *Free Radicals*; Kochi, J. K., Ed.; Wiley: New York, 1973; Chapter 17.
(32) Benson, S. W. *Thermochemical Kinetics*; Wiley: New York, 1976.
(33) Benson, S. W. *J. Am. Chem. Soc.* **1965**, *87*, 972–979.
(34) The model described here assumes a homogeneous liquid phase. Alternatives include heterogeneous liquid phase models in which [O_2(l)] is higher near the gas–liquid interface.

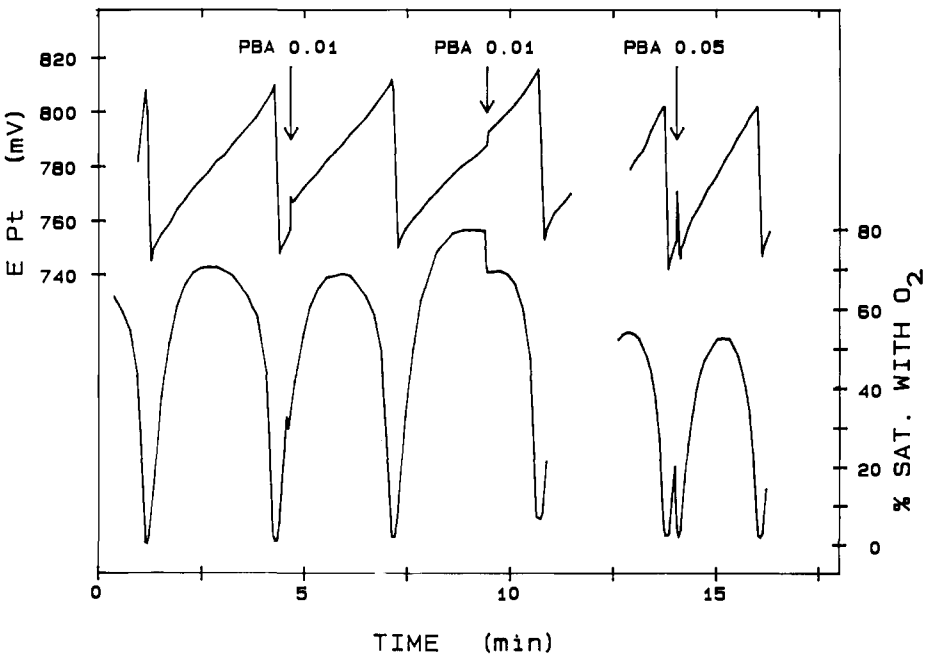

Figure 9. Effect of perbenzoic acid (PBA) additions on the potential of a platinum electrode (upper traces) and dissolved oxygen concentration (lower traces). Peracid stock solution (0.42 M) was added to a batch reaction of 150 mL. Numbers above the arrows indicate the mole ratio of peracid added to total cobalt.

Observations on the Oscillatory System

Bromide Concentration. Oscillations with an amplitude of 1–4 mV are observed in the potential of a bromide ion selective electrode ($Ag/AgBr,Ag_2S$) vs. Ag/AgCl reference (Figure 7). Although there may be factors other than [Br^-] which influence the observed potential (corrosion of the electrode, small changes in the junction potential of the reference electrode), the straightforward interpretation of these changes is that an increase of 1 mV corresponds to a decrease of approximately 3.3% in [Br^-]. Prior to making the measurements of Figure 7, the potential of the Br^--selective electrode was −82.0 mV in a solution containing 10 mM Br^- and 20 mM Co(II) but without benzaldehyde. The potentials during oscillations are similar to this value, and [Br^-] remains near its initial value of 10 mM. These observations are consistent with the small value assigned to the formation constant of a $Co(III)_2Br^-$ complex, K_8.

In the Belousov–Zhabotinsky and other "bromate-driven, bromide-controlled" oscillators, changes in [Br^-] of several orders of magnitude are an essential feature of the mechanism.[35] Thus, the benzaldehyde oscillator is not another example of a bromide-controlled oscillator. Larger fluctuations in [Br^-] have, however, been observed by other investigators. Rastogi and Das[36] found oscillations in this system of about 25 mV in a Ag/AgBr electrode. These would correspond to a change in [Br^-] by a factor of 2.6.

Measurements of Benzaldehyde and Benzoic Acid. If the average dissolved oxygen concentration is appreciably less than saturation, then the rate of oxidation of benzaldehyde can be limited by the mass transfer of oxygen from the gas phase into solution (R17). The rate of disappearance of benzaldehyde, averaged over many oscillatory cycles, was indeed found to be zero order in benzaldehyde with air as the oxidant (details are provided in the supplementary material).

Optical measurements indicate that a substantial (2–20 mM) concentration of Co(III) is reduced to Co(II) during stage II of the oscillation (Figure 1). This occurs through R8 + R13 + R15, with the net transformation B above. The incremental decrease in [PhCHO] from stage II of a single oscillation can be observed. Samples were withdrawn for HPLC analysis at three phases in the cycle: at the beginning, middle, and end of stage I (Figure 8). As the yield of benzoic acid was near unity, the sum of the concentrations of benzaldehyde and benzoic acid serves as an internal standard. The benzaldehyde concentration is then calculated from $[PhCHO] = [PhCHO]_0 \times a/(a + b)$, where $[PhCHO]_0$ is the initial concentration of benzaldehyde and a and b are the measured benzaldehyde and benzoic acid concentrations, respectively. An estimate of the instantaneous rate of benzaldehyde disappearance $d[PhCHO]/dt$ is made from incremental changes in benzaldehyde concentration. The total quantity of benzaldehyde which disappears in stage I (13.5 ± 3 mM for the five oscillations of Figure 8) is similar to the amount (11 ± 3 mM) destroyed in stage II, though the rate is much higher in stage II. The samples for Figure 8 were taken near the end of a batch reaction. There, at the end of stage I, almost all of the 20 mM cobalt is present as Co(III). If the stoichiometry of stage II were that of process B, a maximum of 10 mM of benzaldehyde would be destroyed in stage II, in reasonable agreement with the observations.

Perbenzoic Acid Additions. Large concentrations of perbenzoic acid do not accumulate during the oscillating reaction. An iodine/thiosulfate titration of an aliquot of the oscillating mixture showed no buildup of oxidizing equivalents beyond a small amount easily attributable to Co(III). Thus the concentration of perbenzoic acid is less than 10 mM. Given the high rate of reaction with Co(II) (R1, R2) or Br^- (D3) and the observation that at no time are both Co(II) and Br^- depleted, this is not unexpected. Perbenzoic acid does accumulate during benzaldehyde oxidations catalyzed by low concentrations of cobalt in the absence of bromide.[5] Under those conditions most of the cobalt is present as Co(III), which reacts more slowly with peracid.

Figure 9 shows the potential of a platinum electrode and the dissolved oxygen concentration after addition of perbenzoic acid at 1:100 and 1:20 mole ratios to cobalt. Small quantities of added peracid cause an immediate increase in the potential and a decrease in [O_2(l)], after which stage I continues on its normal course. There were also increases in light absorption at 620 nm due to Co(III). The step increases in potential, and light absorption can be accounted for by R1 and R2. Note that the same quantity of peracid added at a later time in stage I causes a smaller increase in potential, consistent with the Nernst equation. A larger amount of peracid can raise the potential and decrease the oxygen concentration sufficiently to force an immediate transition to stage II. The model R1–R21 reproduces the step increase in potential but does not account for the almost instantaneous drop in dissolved oxygen. Possibly a fraction of the initially formed $Co(III)_2^a$

(35) Noyes, R. M. *J. Am. Chem. Soc.* **1980**, *102*, 4644–4649.
(36) Rastogi, R. P.; Das, I. *Indian J. Chem.* **1984**, *23*, 363–365.

Table III. Experimental Effect of Concentrations in the Feed on the Period τ, the Time from E_{max} to E_{min} (τ_2, or Time for Stage II)[a]

[Co], mM	[Br^-], mM	[PhCHO], mM	τ, s	τ_2, s	E_{max}, mV	ΔE, mV	$[O_2(l)]_{max}$
11	10	750	ss		715		<0.003
11.8	10	750	5	2	713	4	0.003
12.2	10	750	7	3	730	23	0.009
14.1	10	750	10	3	741	36	0.069
20.3	10	750	57	5	782	64	0.31
33.7	10	750	251	13	819	80	0.43
46.1	10	750	367	18	837	86	0.32
85	10	750	174	26	799	31	0.26
99	10	750	86	29	788	13	0.08
102	10	750	ss		780		<0.003
20	3	750	ss		890		<0.002
20	3.4	750	265	82	885	56	0.45
20	6.0	750	98	13	818	68	0.36
20	11.3	750	80	5	781	59	0.36
20	25	750	25	4	739	48	0.11
20	36	750	7.3	3.5	683	14	0.004
20	50	750	ss		685		<0.005
20	10	100	ss		824		0.51
20	10	206	753	16	825	75	0.84
20	10	232	645	14	821	77	0.84
20	10	310	489	13	819	79	0.83
20	10	750	92	6	792	77	0.46
20	10	1000	46	5	772	63	0.19
20	10	1500	11	3	734	32	0.028
20	10	2000	9	4	723	8	0.006
20	10	2700	ss		720		<0.005

[a] E_{max} is the maximum in potential, ΔE is the difference between the maximum and minimum in potential, as the amplitude of oscillations, and $[O_2(l)]_{max}$ is the maximum concentration of dissolved oxygen expressed as a fraction of the saturation value of 6 mM. An entry of ss under τ denotes a steady state.

produces benzoyl radicals before rearranging to $Co(III)_2^s$.

The potential of the bromide-selective electrode rapidly increases from −84 (vs. Ag/AgCl) to −55 mV (decrease in [Br^-] from 10 to 3.3 mM) upon addition of perbenzoic acid in a 1:1 mole ratio to total cobalt. As the peracid is a two-electron oxidant, this is more than enough to oxidize all the cobalt. These rapid initial changes are followed by a slower (12-s) recovery during which bromide ion concentration returns to its initial value. The decrease in bromide ion may be due to oxidation to bromine (D3, D5). The subsequent slow step in which Br^- recovers its normal value might then be a reduction of bromine to bromide with aldehyde going to acid. These observations are consistent with the majority of peracid reacting with Co(II) when the latter is not depleted.

The addition of benzoic acid (0.5 M) had little effect on the amplitudes or period of oscillation measured by the Pt and O_2 electrodes.

Oxygen Labeling. Several oscillatory oxidations were carried out with $^{18}O_2$ (98% isotopic purity) oxidant on the 50-mL scale, and the products were analyzed by GC/MS. The product benzoic acid was found to be 45% singly labeled with ^{18}O; this value had not been decreased by exchange of oxygen between benzoic acid and water. A prediction as to the incorporation of ^{18}O can be made if process A and B are considered the dominant stoichiometries of stage I and stage II, respectively:

$$PhCH^{16}O + {}^{18}O^{18}O + 2Co(II) + 2H^+ \rightarrow PhC^{16}O^{18}OH + Co(III)_2^s + H_2{}^{18}O \quad (A)$$

$$PhCH^{16}O + Co(III)_2^s + H_2{}^{16}O \rightarrow PhC^{16}O^{16}OH + 2Co(II) + 2H^+ \quad (B)$$

Over one oscillatory cycle, the two processes generate equal amounts of benzoic acid. The Co(III) produced by process A is consumed by B. Thus, we would expect the benzoic acid produced to be composed of 50% nonlabeled $PhC^{16}O^{16}OH$ and 50% singly labeled $PhC^{16}O^{18}OH$. More detailed discussions of the oxygen labeling experiments and calculations as well as the observed deviation from 50% are to be discussed in a separate publication.

Concentration Sensitivity. Another test of any mechanistic model, particularly oscillatory models, is to compare the experimental and calculated effects of changing the inputs. In CSTR experiments these constraints may include the residence time in the reactor (liquid volume/liquid flow rate) and the concentrations in the feed. A "phase diagram" is often constructed depicting regions in constraint space of qualitatively different behaviors, such as steady state or oscillation.[37] In steady-state regions an adequate model will describe the stable concentrations and reaction rates. Within the oscillatory regions the experimental and calculated amplitude, shape, and period of oscillation may also be compared as the concentrations are changed. A period vs. concentration plot is expected to be sensitive to the "rate-determining" steps in the mechanism which involve that species.

For each of the four parts below, the input concentration of one species is varied while the others are held constant at the values listed in Table I. A preheated solution containing benzaldehyde and catalyst was pumped into the reactor at a constant rate, while reactor liquid was drained at the same rate. The liquid flow rate to the reactor was 10 mL min^{-1} with a 15-min liquid residence time. The calculations were also done on a CSTR system with the same residence time, reactions R1–R21 from Table I, with only Co(II), Br^-, and PhCHO in the liquid feed.

1. Cobalt Dependence. For [Co] < ~11 mM in the feed the experimental system achieves a steady state characterized by low potential and low $[O_2(l)]$. At [Co] = 12 mM, oscillations begin with small amplitude and period (Figure 10 and Table III). A maximum in period (τ) and amplitude (ΔE, the difference between the extremes of potential) is reached near 50 mM cobalt. Oscillations cease when [Co] exceeds 100 mM, producing a steady state characterized by high potential and low dissolved oxygen concentration.

The calculations of the effect of cobalt concentration (Figure 10 and Table IV) were able to reproduce qualitatively these experimental features:

(a) The calculated steady state at low [Co] is characterized by a low ratio [Co(III)]:[Br^-] = 0.20 and low dissolved oxygen concentration (0.32×10^{-5} of saturation).

(b) The τ vs. [Co] curve is concave downward.

(c) The initial increase of amplitude with increasing [Co] occurs primarily by increasing E_{max} rather than by lowering E_{min}

(37) DeKepper, P.; Boissonade, J. *Oscillations and Traveling Waves in Chemical Systems*; Field, R. J., Burger, M., Eds.; Wiley: New York, 1985; Chapter 7.

Table IV. Calculated Effect of Concentrations in the Feed on τ, τ_2, $[Co(III)]_{max}/[Br^-]$, ΔE, and $[O_2(l)]_{max}$[a]

[Co], mM	[Br⁻], mM	[PhCHO], mM	τ, s	τ_2, s	$[Co(III)]_{max}/[Br^-]$	ΔE, mV	$[O_2(l)]_{max}$
5	10	750	ss		0.20		0.32×10^{-5}
6.2	10	750	34	14	0.48	47	0.028
20	10	750	93	10	1.6	89	0.53
120	10	750	139	8	3.8	37	0.28
220	10	750	60	8	5.2	11	0.055
250	10	750	ss		4.9		0.63×10^{-4}
20	0.5	750	ss		32.0		0.19×10^{-5}
20	0.75	750	57	35	27.0	19	0.10
20	5.0	750	103	13	4.1	59	0.50
20	40	750	41	6	0.17	107	0.25
20	160	750	11	2.8	0.13	69	0.053
20	50	750	2.8	1.3	0.002	26	0.002
20	600	750	ss		0.41×10^{-3}		0.18×10^{-4}
20	10	75	ss		2.0		0.43
20	10	100	460	8	1.4	85	0.89
20	10	1250	47	12	1.1	56	0.19
20	10	1800	22	11	0.43	2	0.56×10^{-5}
20	10	1900	ss		0.39		0.47×10^{-5}

[a] ΔE is calculated from $\Delta E = 78$ mV log $([Co(III)_{max}]/[Co(III)_{min}]$. Other notation is as in Table III.

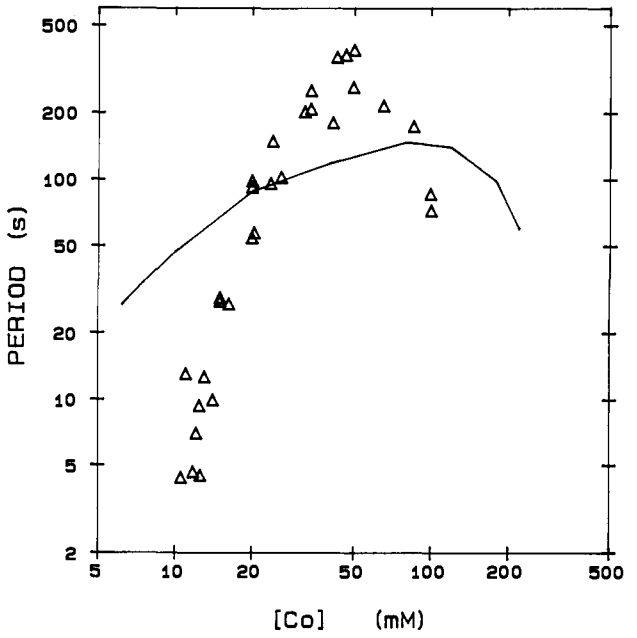

Figure 10. Experimental (triangles) and calculated (lines) effect of cobalt concentration in the feed on the period of oscillation. Steady states are found experimentally or calculated at concentrations outside the interval indicated by the triangles or solid line, respectively.

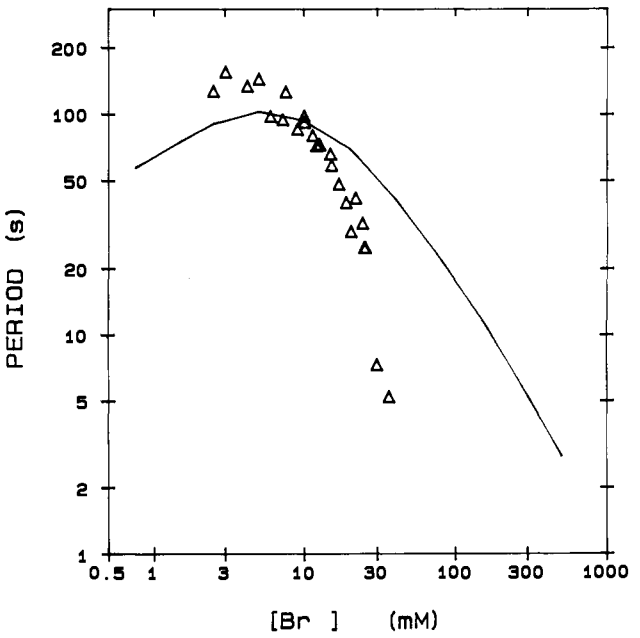

Figure 11. Experimental (triangles) and calculated (lines) effects of bromide concentration in the feed on the period of oscillation.

(d) The calculated steady state at high [Co] has a larger ratio $[Co(III)]:[Br^-] = 4.9$ (higher potential) than the steady state at low [Co].

Two notable differences between calculation and experiment are as follows:

(e) The calculated amplitude and period are too large at low [Co].

(f) The calculated length of stage II (τ_2) decreases with increasing [Co], contrary to increase in experiment.

2. Bromide Dependence. At very low concentrations of bromide, the reaction resembles a cobalt-only catalyzed oxidation of benzaldehyde: the ratio [Co(III)]:Co(II)] is high, the reaction is fast, and $[O_2(l)]$ is depleted (Table III). As $[Br^-]$ is increased, the potential falls, until oscillations begin at $[Br^-] = 3$ mM. The onset of oscillations as $[Br^-]$ increases may be described as a subcritical Hopf bifurcation[38] (also called a "hard" loss of stability[39]), characterized by an abrupt transition from a steady state to oscillations with finite amplitude. In contrast, with increasing cobalt concentration, the oscillations smoothly grow from zero to finite amplitude (supercritical bifurcation or soft excitation). As $[Br^-]$ is increased, the period, amplitude, and $[O_2(l)]_{max}$ all decrease, a behavior pattern similar to that observed with increasing benzaldehyde. Bromide differs from benzaldehyde, in that τ_2 is very long (82 s) at low bromide concentrations. The high-$[Br^-]$ steady state is characterized by low potential and low dissolved oxygen concentration.

The calculations (Figure 11 and Table IV) of the effect of bromide concentration were able to qualitatively reproduce these experimental features:

(a) The calculated steady state at low $[Br^-]$ has a high [Co(III)] and low $[O_2(l)]$.

(b) The subcritical bifurcation to oscillations is reproduced, though it occurs at too low a concentration (0.7 mM calculated, 3 mM experimental).

(c) τ_2 and E_{max}, decrease with increasing $[Br^-]$.

(d) The high-$[Br^-]$ steady state is characterized by low [Co(III)] and $[O_2(l)]$.

The most obvious disagreement is that the calculated rate of decrease of τ with increasing $[Br^-]$ is smaller than the experimental. Also, the calculated high-$[Br^-]$ steady state begins at much higher $[Br^-]$ (>600 mM) than experiment (>50 mM). The competition between R5 and R13 increases the amplitude of the

(38) Marsden, J.; McCracken, M. *The Hopf Bifurcation and its Applications*; Springer-Verlag: New York, 1976; Appl. Math. Sci. 19.

(39) Arnold, V. I. *Catastrophe Theory*; Springer-Verlag: New York, 1984.

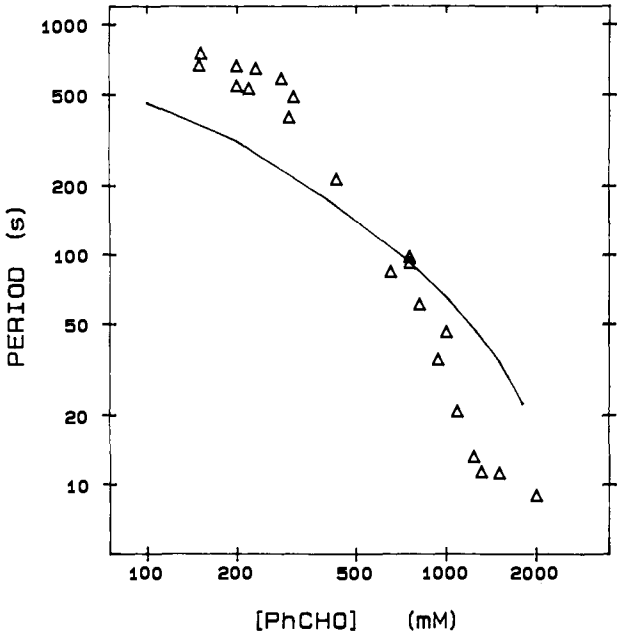

Figure 12. Experimental (triangles) and calculated (lines) effects of benzaldehyde concentration in the feed on the period of oscillation.

$[Co(III)_2^5]$ oscillation at higher $[Br^-]$. The simpler model[2], in which this competition is not dependent on $[Br^-]$, shows the correct slope for the τ vs. $[Br^-]$ plot at high $[Br^-]$. However, it fails to predict the increase in τ_2 at low $[Br^-]$ and diverges to $\tau = \infty$ as $[Br^-]$ is reduced.

3. Benzaldehyde Dependence. The steady state at low [PhCHO] is characterized by a relatively high potential and an intermediate $[O_2(l)]$ (Table III). The oxygen concentration is determined not so much by kinetics as by stoichiometry: the amount of benzaldehyde fed is smaller than the amount of oxygen available from the gas phase. When the benzaldehyde supply is larger, all steady states measured had a very low $[O_2(l)]$. Oxygen absorption is then rate limiting. The occurrence of oscillations, in which $[O_2(l)]$ rises to values comparable to the saturation value of 6 mM, thus leads to a less than maximum rate for benzaldehyde oxidation and incomplete usage of O_2.

Increasing [PhCHO] leads to a subcritical Hopf bifurcation and oscillations at 200 mM. As [PhCHO] increases, τ, $[O_2(l)]_{max}$, E_{max}, and ΔE decrease. Oscillations are not found at aldehyde concentrations greater than 2700 mM, although this limiting concentration increases quickly with higher oxygen flow rates or stirring speeds. The high-[PhCHO] steady state has low potential (pink solution) and low $[O_2(l)]$.

The calculations (Table IV and Figure 12) qualitatively reproduce the experimental data in several features:

(a) The range of oscillations is 100–1800 mM [PhCHO].

(b) The steady state at low [PhCHO] exhibits high [Co(III)] and intermediate $[O_2(l)]$.

(c) The steady state at high [PhCHO] has low [Co(III)] and low $[O_2(l)]$.

(d) τ, E_{max}, and ΔE decrease with increasing [PhCHO].

The major disagreements are that the slope of the τ vs. [PhCHO] plot is smaller than experiment and the calculated τ_2 does not decrease with increasing [PhCHO] as rapidly as observed.

4. Water Dependence. Oscillations were present from about 5% to 20% H_2O, with maximum amplitude near 10% H_2O. The steady states obtained at both high and low water content were characterized by a low dissolved oxygen concentration, indicating that the rate of oxidation was high at these extremes. As water has not been included explicitly in the kinetic model, no comparison with calculation is given.

Conclusions. The chemistry of subsystems of the oscillator was explored, including oxidation of Co(II), reductions of Co(III), oxygen solubility and transport, and reactions occurring only with O_2 present. The rate constants for several of these reactions were measured or estimated from literature data. In the absence of oxygen, benzaldehyde and bromide were found to have a synergistic effect on the reduction of cobalt(III) consistent with a chain process involving oxy-centered radicals. Oscillations occurring in the presence of oxygen involve an autocatalytic production of cobalt(III) coupled to a periodic depletion of dissolved oxygen. The bromide ion concentration does not oscillate appreciably, but alters the rates of reactions of cobalt(III) complexes with the organic compounds. At the standard concentrations (Table I), the period decreases with increasing $[Br^-]$, increasing [PhCHO], or decreasing [Co]. On varying the concentrations, the bifurcation from steady state to oscillations can be of two qualitatively different types. Oxygen labeling shows that there are two major pathways for benzoic acid production, one of which incorporates oxygen from dioxygen and one which incorporates oxygen from water.

A kinetic model combining the reactions of the individual subsystems gives reasonable predictions of the nature of the steady states, the type of bifurcation to oscillation, the region of oscillation in concentration space, and the general dependence of the amplitude and period of concentration. Its most notable deficiency is an underestimation of the magnitude of the slopes of the period vs. concentration plots. The two major pathways for benzoic acid production are easily explained by the model.

The discussion given above has indicated to us the capability of an oscillatory system to provide new information on the mechanism of a complex reaction, even one which previously has been studied extensively under nonoscillatory conditions.[4,5] The limitations of the model suggest that further efforts may yield an even deeper understanding of a prototypical system.

Acknowledgment. We wish to thank Paul A. Berry, John S. Donahue III, and Francis A. Truszkowski for experimental assistance. Richard G. McKay and Fulton Kitson performed the GC/MS analysis for ^{18}O.

Registry No. Benzaldehyde, 100-52-7; cobaltous acetate, 71-48-7; cobalt(III), 22541-63-5; bromide, 24959-67-9.

Supplementary Material Available: Conditions for and rate of reduction of HOBr by PhCHO, potential and spectrophotometric data for Co(II)–Br^- complexes, calculation of Henry's law constant, measurement of O_2 equilibration time, and [PhCHO] decay curves for oscillator in the batch mode (13 pages). Ordering information is given on any current masthead page.